

Predicting trends in atmospheric CO₂ across the Mid-Pleistocene Transition using existing climate archives

Jordan R.W. Martin¹, Joel Pedro^{2,3}, Tessa R. Vance³

¹Institute for Marine and Antarctic Studies, University of Tasmania, Hobart, 7004, Australia

²Australian Antarctic Division, Kingston, 7050, Australia

³Australian Antarctic Program Partnership, Institute for Marine and Antarctic Studies, University of Tasmania, Hobart, 7004, Australia

Correspondence to: Jordan R.W. Martin (jrmartin@utas.edu.au)

Abstract

During the Mid-Pleistocene Transition (MPT), ca. 1200–800 thousand years ago (kya), the Earth's glacial cycles changed from 41 kyr to 100 kyr periodicity. The emergence of this longer ice-age periodicity was accompanied by higher global ice volume in glacial periods and lower global ice volume in interglacial periods. Since there is no known change in external orbital forcing across the MPT, it is generally agreed that the cause of this transition is internal to the earth system. Resolving the climate–carbon cycle–cryosphere dynamics processes responsible for the MPT remains a major challenge in earth and palaeoclimate science. To address this challenge, the international ice core community has prioritized recovery of an ice core record spanning the MPT interval. The data from such 'oldest ice' projects are still several years away.

Here we present results from a simple generalized least squares model that predicts atmospheric CO₂ out to 1.5 Myr. Our prediction utilises existing records of atmospheric carbon dioxide (CO₂) from Antarctic ice cores spanning the past 800 kyr along with the existing LR04 benthic $\delta^{18}\text{O}_{\text{calcite}}$ stack (Lisiecki & Raymo, 2005) from marine sediment cores. Our predictions assume that the relationship between CO₂ and benthic $\delta^{18}\text{O}_{\text{calcite}}$ over the past 800 thousand years can be extended over the last one and a half million years. The implicit null hypothesis is that there has been no fundamental change in feedbacks between atmospheric CO₂ and the climate parameters represented by benthic $\delta^{18}\text{O}_{\text{calcite}}$, global ice volume and ocean temperature.

We test the GLS-model predicted CO₂ concentrations against observed blue ice CO₂ concentrations, $\delta^{11}\text{B}$ -based CO₂ reconstructions from marine sediment cores and $\delta^{13}\text{C}$ of leaf-wax based CO₂ reconstructions (Higgins *et al.*, Yan *et al.*, 2019 and Yamamoto *et al.*, 2022). We show that there is not clear evidence from the existing blue ice or proxy CO₂ data to reject our predictions nor our associated null-hypothesis. A definitive test and/or rejection of the null hypothesis may be provided following recovery and analysis of continuous oldest ice core records from Antarctica, which is still several years away. The record presented here should provide a useful comparison for the oldest ice core records and opportunity to provide further constraints on the processes involved in the MPT.

39 **1 Introduction**

40 Ice core records from Antarctica provide comprehensive and continuous records of many climate parameters
41 over the last 800 thousand years, e.g. from the Vostok (Petit *et al.*, 1999) and European Project for Ice Coring in
42 Antarctica's Dome-C (EDC) ice cores (Jouzel *et al.*, 2007). One of the major challenges in climate science lies
43 beyond the current threshold of the ice core record. The Mid-Pleistocene Transition (MPT) spans from ca.
44 1200–800 thousand years ago (kya) (Chalk *et al.*, 2017) and is characterised by a change from regularly paced
45 40 thousand year (kyr) glacial cycles with thinner glacial ice sheets to quasi-periodic 100 kyr glacial cycles in
46 which ice sheets are more persistent and thicker (Clark *et al.*, 2006, Chalk *et al.*, 2017). To resolve the forcings
47 and feedbacks involved in this transition, multiple nations are targeting recovery of continuous ice cores
48 spanning the MPT under the framework of the International Partnerships in Ice Core Science (IPICS) oldest ice
49 core challenge (IPICS, 2020).

50

51 The purpose of the current study is to make a simple prediction of atmospheric CO₂ across the MPT. Cross-
52 comparison of our and other predicted CO₂ records against observed MPT CO₂ data will aid in testing
53 competing hypotheses on the cause of the transition, in particular the role of carbon cycle changes.

54

55 The MPT occurred in the absence of any changes to orbital insolation forcing, therefore, the mechanisms behind
56 the MPT must be internal to the earth system (Raymo, 1997; Ruddiman *et al.*, 1989). Multiple hypotheses have
57 been put forward to explain the transition. A common element in many of these, is internal climate/earth system
58 changes which allow for the development of thicker, more extensive ice sheets that could endure insolation
59 peaks corresponding to the 23 kyr precession and 41 kyr obliquity cycles, i.e., an increase in the threshold for
60 deglaciation and altered sensitivity to orbital forcings (Tzedakis *et al.*, 2017; McClymont *et al.*, 2013). Among
61 the prominent hypotheses are the following three.

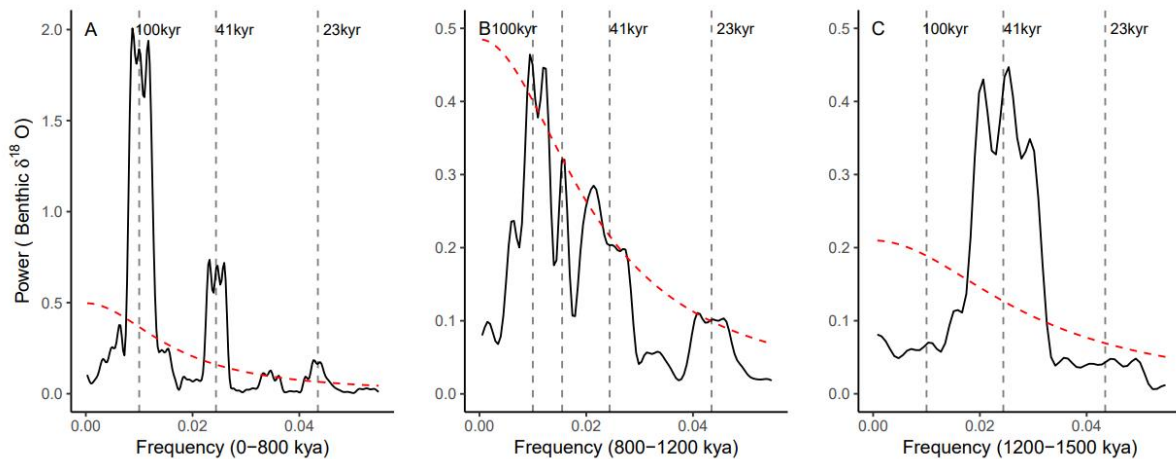
- 62 1) A long term decrease in radiative forcing due to a secular reduction in atmospheric CO₂ across the
63 transition (e.g. Berger *et al.*, Hönisch *et al.*, 2009; 1999, Raymo *et al.*, 1988). According to this view,
64 reduced radiative forcing drives the formation of larger and more stable ice sheets.
- 65 2) Progressive removal of sub-glacial regolith during the 41 kyr glacial cycles. Clark & Pollard (1998)
66 proposed that ice sheet basal sliding prior to the MPT was enhanced by the presence of a low-friction
67 sedimentary regolith layer between the Laurentide ice sheet and the crystalline bedrock. According to
68 this view, progressive removal of this sedimentary layer then favored the development of larger and
69 more persistent post-MPT ice sheets.
- 70 3) Phase-locking of the Northern and Southern Hemisphere ice sheets. In frequency spectra of the global
71 marine benthic $\delta^{18}\text{O}$ record (Fig. 1) there is no evidence of the precession (23 kyr) component of
72 northern hemisphere insolation prior to the MPT; the spectra is dominated by the obliquity (41 kyr)
73 component (Fig. 1C). Emergence of significant precession and eccentricity signals occurs across the
74 MPT (Fig. 1B), and all three components are clearly present after the MPT (Fig. 1A). Raymo *et al.*
75 (2006) suggested that precession-paced changes in northern and southern hemisphere ice volumes may
76 have occurred prior to the MPT, but are cancelled due to out-of-phase ice volume changes between the
77 two hemispheres (Raymo & Huybers, 2008). According to this view, during the MPT the precession-
78 paced changes to fall into phase between the two hemispheres, such that the precession signal emerges

79 (Raymo *et al.*, 2006). In this view the global synchronization of ice volume drives the formation of
80 larger and more stable ice sheets.

81

82 These hypotheses are not mutually exclusive. For a recent review on the cause of the MPT see Berends *et al.*
83 (2021).

84



85

86

87 **Figure 1: Thomson Multi-taper Method (MTM) spectral analysis representing relative power of signal periodicity for:**
88 **A) Benthic $\delta^{18}\text{O}$ stack after (0–800 kya) the Mid-Pleistocene Transition (MPT); B) Benthic $\delta^{18}\text{O}$ across the MPT (800–**
89 **1200 kya); C) Benthic $\delta^{18}\text{O}$ prior to the onset of the MPT (1200 kya–1500 kya). Each with a robust AR (1) 95 %**
90 **Confidence interval (red dashed line). Benthic $\delta^{18}\text{O}$ stack data from Lisiecki and Raymo (2005).**

91

92 For a long term decrease in radiative forcing by atmospheric CO_2 to be the cause of the MPT, the reduction in
93 CO_2 would be expected in both glacial and interglacial stages (Chalk *et al.*, 2017). However, low resolution
94 boron-isotope-based CO_2 reconstructions by Hönisch *et al.*, (2009), and Chalk *et al.*, (2017) suggest that glacial-
95 stage CO_2 drawdown occurred over the MPT in the absence of interglacial CO_2 drawdown. Glacial-stage CO_2
96 draw-down across the MPT may be a positive climate-carbon cycle feedback to changes in ice sheet dynamics,
97 including CO_2 drawdown by enhanced iron fertilisation of the Southern Ocean in response to exposed
98 continental shelves due to lower sea level, as well as planetary drying associated with colder climate conditions
99 (Chalk *et al.*, 2017). Colder glacial temperatures that enhance the solubility of CO_2 in the oceans, and reduced
100 abyssal ocean ventilation has also been implicated in enhanced glacial-stage ocean storage of CO_2 (McClymont
101 *et al.*, 2013; Hasenfratz *et al.*, 2019).

102

103 Testing of hypotheses on the cause of the MPT is currently limited by the lack of a continuous ice core that
104 spans its duration. The International Partnership in Ice Core Sciences (IPICS) has nominated recovery of such a
105 record as a key priority in ice core research (IPICS, 2020). Multiple national and international projects have
106 commenced, or are soon to commence, drilling for ‘oldest ice’ (see e.g. Shugi, 2022). In this project, we take
107 inspiration from the “EPICA Challenge” in which the paleoclimate and modeling community was challenged to
108 predict the global atmospheric carbon dioxide and methane concentrations from 800–400 kya based on the
109 existing 400 kyr Vostok ice core record (Wolff *et al.*, 2004). Here, we use a generalised least squares (GLS)

110 model trained on continuous climate archives to predict a CO₂ record out to 1.5 Mya. We utilise two primary
111 data sets for the GLS model: the existing 800 kyr ice core composite record of atmospheric CO₂ (Bereiter *et al.*,
112 2015) and the LR04 benthic stack of 52 globally-distributed records of the ¹⁸O to ¹⁶O ratio of fossil benthic
113 foraminifera calcite (hereafter referred to as the LR04 $\delta^{18}\text{O}$ benthic stack). The $\delta^{18}\text{O}$ ratios in the LR04 benthic
114 stack are governed by ocean temperature and global ice volume at the time the foraminifera lived, with higher
115 values indicating both increased ice volume and a colder climate.

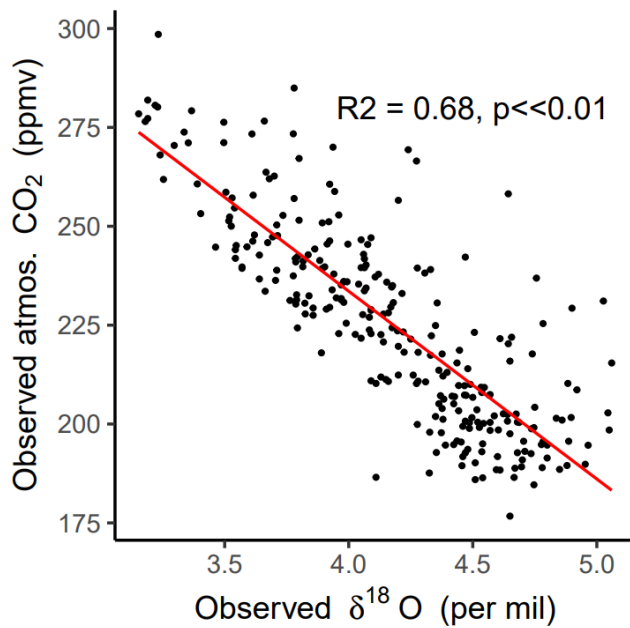
116

117 Fig. 2 shows a scatter-plot of the LR04 $\delta^{18}\text{O}$ benthic stack versus observed ice core CO₂ over the past 800 kyr.
118 Both data sets are binned to equivalent 3-kyr time steps (Methods). The Pearson's correlation coefficient (r)
119 between the data sets is -0.82 ($p < 0.05$) indicating that ~68% of the variance in observed CO₂ is shared with the
120 LR04 $\delta^{18}\text{O}$ benthic stack. This strong relationship provides an initial rationale for using the LR04 $\delta^{18}\text{O}$ benthic
121 stack as an input parameter to predict CO₂ beyond 800 kyr. Mechanistically, multiple processes are expected to
122 contribute to the shared variance. A first order factor is the dependency of CO₂ solubility on ocean temperature
123 (e.g. Millero, 1995). From the simple solubility perspective, colder climate states with increased ice volume and
124 colder ocean temperatures will drive increased ocean uptake of CO₂ (Berends *et al.*, 2021). However, the
125 solubility effect only accounts for a portion of observed glacial CO₂ drawdown (Archer *et al.*, 2000). Multiple
126 additional contributors to the shared variance are proposed in the literature. These include (not exhaustively),
127 direct radiative forcing of ice volume changes by CO₂ (e.g. Shackleton *et al.*, 1985); the impact of ice
128 volume/sea level changes on atmospheric CO₂ via ocean productivity and carbonate chemistry changes (e.g.
129 Broecker, 1982; Archer *et al.*, 2000; Ushie and Matsumoto, 2012); CO₂ drawdown during periods of high ice
130 volume by increased iron fertilization (e.g. Röthlisberger *et al.*, 2004; Martinez-Garcia *et al.*, 2014) and
131 enhanced sea ice extent during periods of high ice volume capping the ventilation of CO₂ from the ocean
132 interior at high latitudes (Stephens and Keeling, 2000).

133

134 A quantitative separation and attribution of the processes linking global ice volume, ocean temperature and
135 atmospheric CO₂ on millennial to orbital timescales is not currently available (e.g. Archer *et al.*, 2000; Sigman
136 *et al.*, 2010; Gottschalk *et al.*, 2019) and will not be attempted here. Rather, we make the simple assumption that
137 the relationships between the LR04 benthic $\delta^{18}\text{O}$ stack and CO₂ can be extended beyond 800 kya and use
138 regression modelling between benthic $\delta^{18}\text{O}$ and CO₂ to make a predictions of CO₂ spanning 800–1500 kya. The
139 deliberately simple implicit assumption, and null hypothesis, is that there is no change to the feedback processes
140 linking benthic $\delta^{18}\text{O}$ and CO₂ before and after the MPT.

141



142 **Figure 2: Scatter plot of the composite observed atmospheric CO₂ record (Bereiter *et al.*, 2015) against**
 143 **the LR04 benthic stack of marine δ¹⁸O records (Lisiecki & Raymo, 2005). Red line is a linear line of best**
 144 **fit ($R^2 = 0.68$; $p < 0.05$).**

145
146

147 To test the null hypothesis, in advance of the recovery of a continuous ice core, we compare our predicted CO₂
 148 record to two sets of low-resolution ice core data that exist outside the current 800 kyr observed CO₂. These data
 149 come from direct CO₂ measurements from ancient “blue ice” from the Allan Hills in East Antarctica (hereafter
 150 referred to as BI-CO₂) from ca. 1 Mya (Higgins *et al.*, 2015) and 1.5 Mya (Yan *et al.*, 2022). We use the term
 151 blue ice to describe deep, ancient glacial ice that has been brought nearer to the surface of an ice sheet by ice
 152 flow. Blue ice is sampled by cutting trenches or shallow drilling of up to several hundred meters (e.g. Higgins *et*
 153 *al.*, 2015). The vertical migration of blue ice is associated with high deformation making the ice samples
 154 stratigraphically complex and hard to date (Higgins *et al.*, 2015). As a result, blue ice records alone do not
 155 provide a continuous CO₂ record across the MPT. We also compare our predicted record to existing proxy-CO₂
 156 reconstructions from boron-isotope analysis of benthic foraminifera in marine sediment records (Chalk, *et al.*,
 157 2017; Dyez *et al.*, 2018; Guillermic *et al.*, 2022), leaf wax δ¹³C carbon isotope ratios (Yamamoto *et al.*, 2022)
 158 and predictions from previous models of various complexities (van de Wal *et al.*, 2011; Willeit *et al.* 2019). We
 159 conclude with discussion of the implications of our results and data-comparisons for the understanding MPT
 160 dynamics.

161

162 **2 Methods**

163 We use a generalised least squares (GLS) model to predict atmospheric CO₂ from the LR04 benthic δ¹⁸O stack
 164 (Fig. 3A and B). We apply an AR(1) correlation factor to account for autocorrelation in the data. The AR(1)
 165 correlation factor yielded the lowest Akaike information criterion (AIC) value from a test of multiple correlation
 166 factors. To obtain common time steps and resolution between the predictor (LR04 benthic δ¹⁸O stack) and
 167 response (CO₂) variables, we re-grid the LR04 benthic stack and Bereiter *et al.*, (2015) CO₂ data into time bins

168 with a resolution of 3-kyr. The GLS regression model was applied over the 0–800 kyr range of the predictor and
169 response variables as follows:

170

$$171 \quad CO_2 = 33.37 \times \delta^{18}O + 365.15, \text{ autoregressive (AR) factor: } 1$$

172

173 Based on the regression model, the $\delta^{18}O$ values of the LR04 Benthic Stack from 800 – 1500 kya were used to
174 predict CO_2 concentration over this range (hereafter referred to as PRED- CO_2). To estimate the GLS model
175 uncertainty and sensitivity we took a bootstrap approach, selecting a random 50% subset of our data and re-
176 running the model 1000 times to determine 95% confidence intervals for the predictions.

177

178 Uncertainties in the independent age scales of both the LR04 stack and the compiled CO_2 record are inherited by
179 our GLS model and its predictions. The LR04 stack includes 57 globally-distributed benthic $\delta^{18}O$ sediment core
180 records. The age models for these cores are independently constructed from the average sedimentation rates of
181 each core, assuming global sedimentation rates have remained relatively stable, and with tuning to a simple ice
182 model based on 21 June insolation at 65°N (Lisiecki & Raymo, 2005). The authors estimate uncertainty of 6 kyr
183 from 1.5 – 1.0 Mya and 4 kyr from 1 – 0 Mya (Lisiecki & Raymo, 2005). The observed CO_2 composite ice core
184 record for the past 800 kya (Bereiter et al., 2015) uses six independent dating methods for various core locations
185 both spatially across Antarctica, and stratigraphically for different sections of the same core. The age uncertainty
186 in the gas timescale has a median over the 0 – 800 kya interval of 2 kyr, but individual uncertainties can reach
187 up to 5 kyr (Veres et al 2013; Bazin et al., 2013). The relative age uncertainties between these input variables
188 may diminish the regression or in some instances lead to spurious correlation. However, we expect any such
189 effects are minor on the basis that our predictions show little sensitivity to the bootstrap analysis with 1000
190 iterations of re-computing the regression after removing 50% of data (see Fig. 3B, C and Discussion).

191

192 **3 Results**

193 Fig. 3B shows the time series of our LR04 benthic $\delta^{18}O$ stack-based GLS model predictions of atmospheric CO_2
194 (PRED- CO_2) over the past 800 kyr, in comparison to the observed ice core CO_2 record from Bereiter et al.,
195 (2015). The correlation coefficient (r^2) between the predicted and observed records is 0.68 ($p \ll 0.01$). Our
196 PRED- CO_2 record out to 1.5 Mya is also shown, overlain with observed Allan Hills blue ice CO_2 (BI- CO_2)
197 datasets of age 1000 ± 89 kya (Higgins et al., 2015) and $1.5 \text{ Mya} \pm 213$ kyr (Yan et al., 2022).

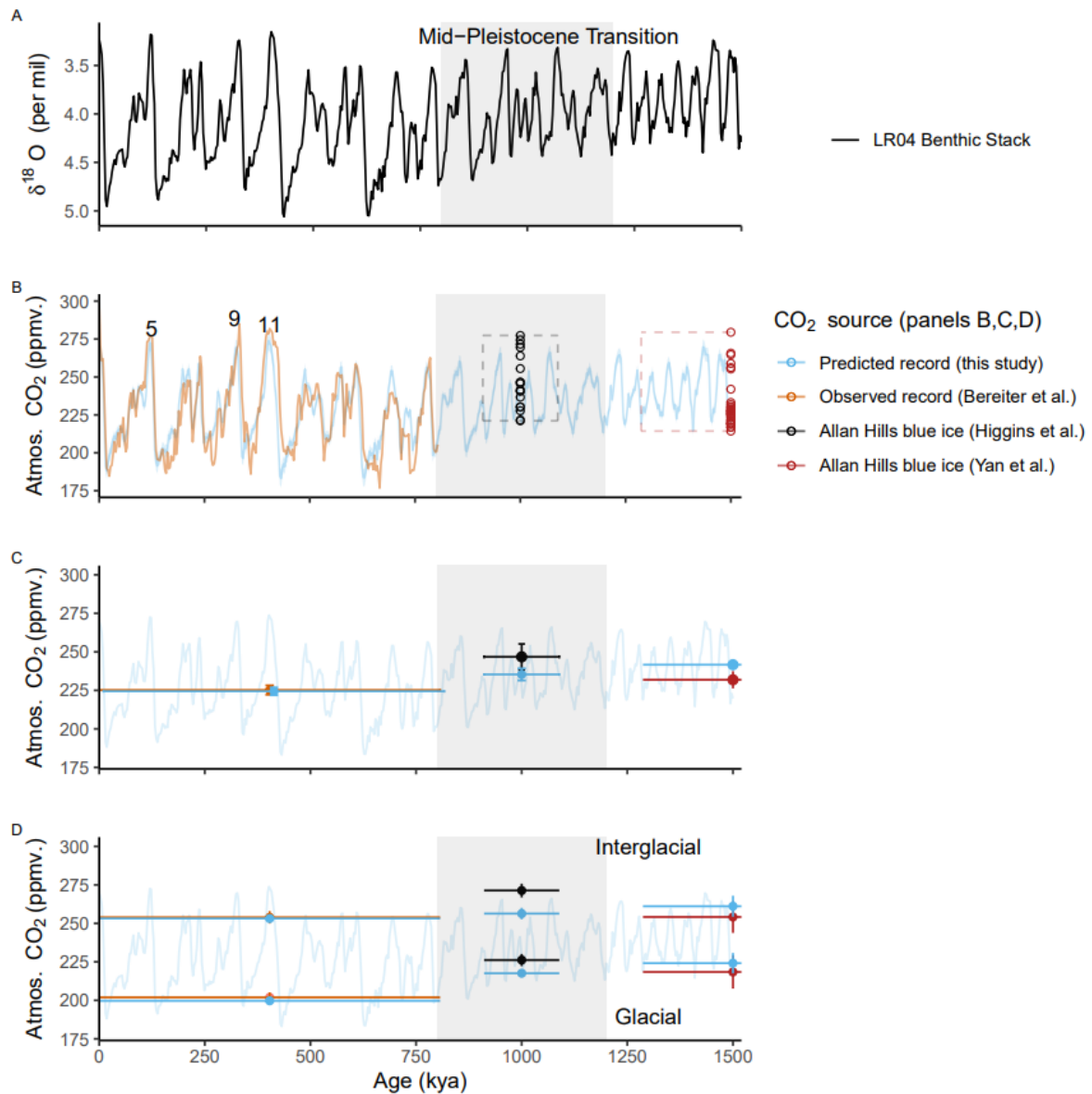
198

199 We evaluate the PRED- CO_2 record against the observed CO_2 data according to criteria of mean concentrations
200 across the common intervals, and mean concentrations in the glacial and interglacial subsets of the data. First,
201 the mean CO_2 concentration over the common intervals (Fig 3C). From 0–800 kya the mean concentration in
202 observed (Bereiter et al., 2015) and PRED- CO_2 data are in close agreement (225.2 ± 3.03 ppm versus the
203 predicted 225.1 ± 2.5 ppm respectively; uncertainties are 95% confidence intervals, i.e. 1.96σ). In the 1000 ± 89
204 kya interval (i.e. averaged across the age uncertainty of the Higgins (2015) blue ice data) the BI- CO_2
205 concentration is ~ 11ppm higher than PRED- CO_2 (246.7 ± 8.4 ppm versus the predicted 235.5 ± 3.9 ppm), this
206 difference is not significant at the 95% confidence level. For the $1.5 \text{ Mya} \pm 213$ kyr interval, the mean BI- CO_2
207 concentration is ~10 ppm lower than PRED- CO_2 (231.9 ± 5.6 ppm versus the predicted 241.7 ± 2.5 ppm),

208 which is marginally significant at the 95% level. Comparisons of mean levels across intervals spanning multiple
209 glacial and interglacial cycles may be biased if (as is likely) the blue ice data is not sampling glacial and
210 interglacial values with the same uniformity as a continuous record.

211

212 To address this, we define the glacial and interglacial thresholds of PRED-CO₂ to be respectively the lower and
213 upper 25th percentiles of the LR04 δ¹⁸O predictor variable (following Chalk *et al.*, 2017). Filtering the observed
214 (Bereiter *et al.*, 2015) CO₂ record and our predicted CO₂ record according to these definitions we find a very
215 close match for glacial (202.0 ± 3.2 versus the predicted 199.7 ± 1.7 ppm) and interglacial intervals (253.9 ± 4.1
216 ppm versus the predicted 253.1 ± 2.3 ppm), over the past 800 kya (see Fig. 3D). For blue ice (BI-CO₂) data, a
217 corresponding LR04 isotope signal could not be confidently applied to the measured CO₂ concentration due to
218 the uncertainties associated with blue ice aging; therefore, we defined the glacial and interglacial thresholds of
219 blue ice data according to the top (interglacial) and bottom (glacial) 25th percentiles of actual CO₂. Applying this
220 to the 1000 ± 89 kya interval finds that observed BI-CO₂ data is ~ 9 ppm higher than PRED-CO₂ during the
221 glacial stages (226.2 ± 4.0 ppm versus the predicted 217.6 ± 2.3 ppm) and ~ 15 ppm higher than PRED-CO₂
222 during the interglacial stages (271.3 ± 4.5 versus the predicted 256.3 ± 3.8 ppm). These differences are
223 significant with respect to the constrained uncertainties. In contrast, during the $1.5 \text{ Mya} \pm 213 \text{ kyr}$ interval, the
224 mean BI- CO₂ concentration is not significantly different to PRED-CO₂ in either glacial (217.6 ± 2.3 versus the
225 predicted 224.2 ± 6.6 ppm) or interglacial stages (256.3 ± 3.8 versus the predicted 261.1 ± 6.3 ppm). These
226 comparisons, particularly the agreement at 1.5 Myr, indicate that PRED-CO₂ is not drifting systematically away
227 from the existing observed BI-CO₂ data. In our view the disagreement at 1.0 Myr, where BI-CO₂ is elevated
228 with respect to PRED-CO₂, does not give sufficient cause to reject the GLS model, it could of course be a
229 failing in the model and/or could be due to potential biases in the blue ice data, for example elevated CO₂
230 concentrations due to in-situ CO₂ production in blue ice (see Discussion).



231
 232 **Figure 3: A) The LR04 Benthic Stack of 57 globally distributed $\delta^{18}\text{O}$ records (Lisiecki & Raymo, 2005).**
 233 **B) Comparison of our PRED-CO₂ (ppm) record to the current continuous composite record (0–800 kya);**
 234 **and to direct CO₂ measurements from Allan Hills blue ice cores (BI-CO₂) ca. 1 Mya (± 89 kyr) (Higgins *et al.*,**
 235 ***2015*) and ca. 1.5 Mya (± 213 kyr) (Yan *et al.*, 2022). Age uncertainty boundaries for the BI-CO₂ data**
 236 **are represented by dashed box boundaries. Marine isotope stages 5, 9, and 11 are numbered on the plot**
 237 **according to Lisiecki & Raymo (2005). C) Mean concentrations of the PRED-CO₂ and observed**
 238 **composite CO₂ records over the range of the observed composite record (offset for clarity), and the mean**
 239 **concentrations of the PRED-CO₂ and BI-CO₂ data at 1 Mya and again at 1.5 Mya averaged over the age**
 240 **uncertainty range of each BI-CO₂ data set. D) As for C) however filtered by the upper and lower 25th and**
 241 **75th percentiles to estimate glacial and interglacial periods.**

242
 243 We now consider long-term trends in interglacial and (separately) glacial CO₂ levels across the past 1.5 Myr in
 244 PRED-CO₂ and in the existing ice core CO₂ data. For PRED-CO₂ there is no significant difference between CO₂
 245 concentrations in the interglacial stages of the 1.5 Mya ± 213 kya, 1000 ± 89 kya and 0–800 kya windows (Fig 4

246 D, blue bars). In the ice core observations, interglacial levels at 1.5 Mya in BI-CO₂ are also within the
247 uncertainties of those in the 0–800 kya interval. Notably, the BI-CO₂ concentrations in the 1000 ± 89 kya
248 interval appear elevated with respect to the 0–800 kyr and 1.5 Mya ± 213 kya intervals, however this elevated
249 (ca. 271 ppm) level is consistent with the observed interglacial CO₂ concentration during interglacials 5, 9 and
250 11 (Fig 3B). Overall, there is no indication in the observed ice core CO₂ data or in PRED-CO₂ for a long-term
251 trend in *interglacial* CO₂ levels across the past 1.5 Myr.

252

253 In comparison, there are significant declines in glacial CO₂ levels across the MPT in PRED-CO₂ and the
254 observed ice core data. For PRED-CO₂, glacial CO₂ concentrations are not significantly different during the 1.5
255 Mya ± 213 kya and 1000 ± 89 kya windows. However, across the MPT, PRED-CO₂ glacial concentrations drop
256 by ~18 ppm. This pattern is consistent with the observed data, where glacial CO₂ levels are also not significantly
257 different between the 1.5 Mya ± 213 kya and 1000 ± 89 kya windows (217.6 ± 2.3 and 226.2 ± 4.0 ppm,
258 respectively) and then fall by 24 ppm to the 0–800 kyr observed glacial mean of 202.0 ± 3.2 ppm. Glacial-stage
259 draw-down of CO₂ across the MPT in the absence of interglacial draw-down is consistent with previous
260 observations based on the boron-isotope-based CO₂ reconstructions (e.g., Chalk *et al.*, 2017; Hönisch *et al.*,
261 2009 and see Discussion). In the following section we also compare PRED-CO₂ data to boron-isotope-based and
262 other CO₂ proxy records covering the 0 to 1.5 Myr interval.

263

264 **4 Discussion**

265 Our objective with this manuscript was to generate the simplest reasonable model to predict CO₂ from the LR04
266 δ¹⁸O benthic stack and to test the predictions against available observations. It is possible that the fit between
267 observed and our predicted CO₂ data could be further improved using a non-linear approach. However, we
268 refrain from a non-linear approach for several key reasons. First, a scatter plot of the LR04 δ¹⁸O benthic stack
269 versus observed ice core CO₂ over the past 800 kyr yields a Pearson's correlation coefficient (R) of -0.82 (Fig.
270 2), indicating that ~68% of the variance in observed CO₂ is shared with the benthic stack. Importantly, there is
271 no evidence in this scatter plot for departure from the linear relationship at high or low CO₂ or benthic δ¹⁸O
272 levels. Second, following the approach of Chalk *et al.*, 2017 and interpreting the upper 25th percentile of CO₂
273 data as representing mean interglacial stage CO₂ and the lower 25th percentile of CO₂ data as representing mean
274 glacial stages CO₂ levels, we see that our predicted interglacial mean value for the past 800 kyr (253.1 ± 2.3
275 ppm) closely overlaps with the observed interglacial mean value (253.9 ± 4.1 ppm) and similarly, the predicted
276 glacial stage mean (199.7 ± 1.7 ppm) closely overlaps with the observed glacial stage mean (202.0 ± 3.2 ppm).
277 Third, the predictions are remarkably insensitive to bootstrap analysis in which 50 % of that data are omitted
278 with each iteration of the GLS model (Fig 1). Such insensitivity to the bootstrap analysis and accurate prediction
279 of glacial *and* interglacial state CO₂ values would be unlikely in the case of major non-linear dependencies
280 between the LR04 predictor and CO₂ response variables. Fourth, non-linear approaches would risk generating
281 an improved fit due to statistical artefacts that do not meaningfully relate to any dependence between benthic
282 δ¹⁸O and CO₂. Finally, the specific causes and sources and sinks involved in glacial to interglacial and
283 millennial-scale CO₂ variations still remain poorly constrained (e.g. Archer *et al.*, 2000; Sigman *et al.*, 2010;
284 Gottschalk *et al.*, 2019). Given this process-uncertainty, the GLS model fits our criteria of the simplest
285 reasonable model. Further, the use of benthic δ¹⁸O to predict atmospheric CO₂ has precedence; in response to

286 the EPICA challenge (Wolff et al., 2004), N. Shackleton used this method to predict atmospheric CO₂ out to 800
287 kyr (Wolff, 2005). Furthermore, inverse modelling of CO₂ forced by the LR04 benthic stack has been
288 undertaken by Berends et al. (2021a) and van de Wal et al. (2011).

289

290 There are several caveats with blue ice data that may affect its use to evaluate our GLS model predictions. The
291 blue ice data may have been subject to diffusional smoothing of CO₂ (e.g. Yan *et al.*, 2019), which would act in
292 the direction of elevating the (lower 25th percentile) assumed glacial concentrations above the glacial
293 atmospheric values and reducing the (upper 25th percentile) assumed interglacial concentrations. There is also
294 the potential for artificially elevated CO₂ concentrations in blue ice due in-situ respiration of CO₂ due to
295 microbial activity in detrital matter. Respiration effects are screened for by measurements of $\delta^{13}\text{C}$ of CO₂,
296 however it is difficult to demonstrate that all samples are unaffected (Yan *et al.*, 2019). These uncertainties
297 support our argument that the GLS-model predictions are not rejected by the available observed BI-CO₂ data.

298

299 We consider the BI-CO₂ data to provide the most reliable measurements of CO₂ concentration, in the absence of
300 a continuous ice core record across the MPT. However, further comparison of our CO₂ predictions can also be
301 made against CO₂ proxy data from non-ice core archives (Fig 4A). We consider here $\delta^{11}\text{B}$ -based atmospheric
302 CO₂ reconstructions (Chalk *et al.*, 2017, Dyez *et al.* 2018 and Guillermic *et al.* 2022) and a recent atmospheric
303 CO₂ reconstruction from $\delta^{13}\text{C}$ of leaf wax (Yamamoto *et al.*, 2022). The continuous $\delta^{11}\text{B}$ -based reconstructions
304 of Dyez *et al.*, (2018) overlap PRED-CO₂ from ~1.38 – 1.5 Mya while the Chalk *et al.*, (2017) reconstruction
305 overlaps PRED-CO₂ from 1.09 – 1.43 Mya. Discrete reconstructions from Guillermic *et al.* (2022) are
306 distributed non-uniformly across the 800 to 1.5 Mya interval. For the two continuous $\delta^{11}\text{B}$ -based reconstructions
307 (Chalk *et al.*, (2017) and Dyez *et al.*, (2018)) the glacial CO₂ levels appear consistent with the PRED-CO₂
308 record, within their reported 30 – 60 ppm uncertainties. However, $\delta^{11}\text{B}$ -based interglacial stages in these
309 reconstructions exceed those of the PRED-CO₂ record (Fig. 4A). The Guillermic *et al.* (2022) reconstructions
310 suggest a larger range of CO₂ concentrations than the overlapping intervals of PRED-CO₂ and of the two
311 continuous $\delta^{11}\text{B}$ -based reconstructions (Fig. 4A). The large range of the Guillermic *et al.* (2022) data and the
312 high interglacial maxima in the Chalk *et al.* (2017) and Dyez *et al.*, (2018) data, all significantly exceed the
313 range and interglacial maxima from the BI-CO₂ estimates. These discrepancies internally between different
314 $\delta^{11}\text{B}$ -based CO₂ reconstructions and between the $\delta^{11}\text{B}$ -based reconstructions and the BI-CO₂ data, may be due to
315 uncertainties associated with the $\delta^{11}\text{B}$ proxy transfer function. The $\delta^{11}\text{B}$ -based CO₂ reconstructions are
316 dependent on assumptions about multiple components of the carbonate system, including local marine carbon
317 chemistry and the CO₂ saturation state in the past and (Hönisch *et al.*, 2009). Evidence that $\delta^{11}\text{B}$ -based
318 reconstructions may overestimate interglacial stage CO₂ is also seen in data from Chalk *et al.*, (2017) spanning
319 ca. 0–250 kya, where the $\delta^{11}\text{B}$ -based interglacial CO₂ levels exceed the continuous ice core CO₂ record by ca. 30
320 ppm (not shown).

321

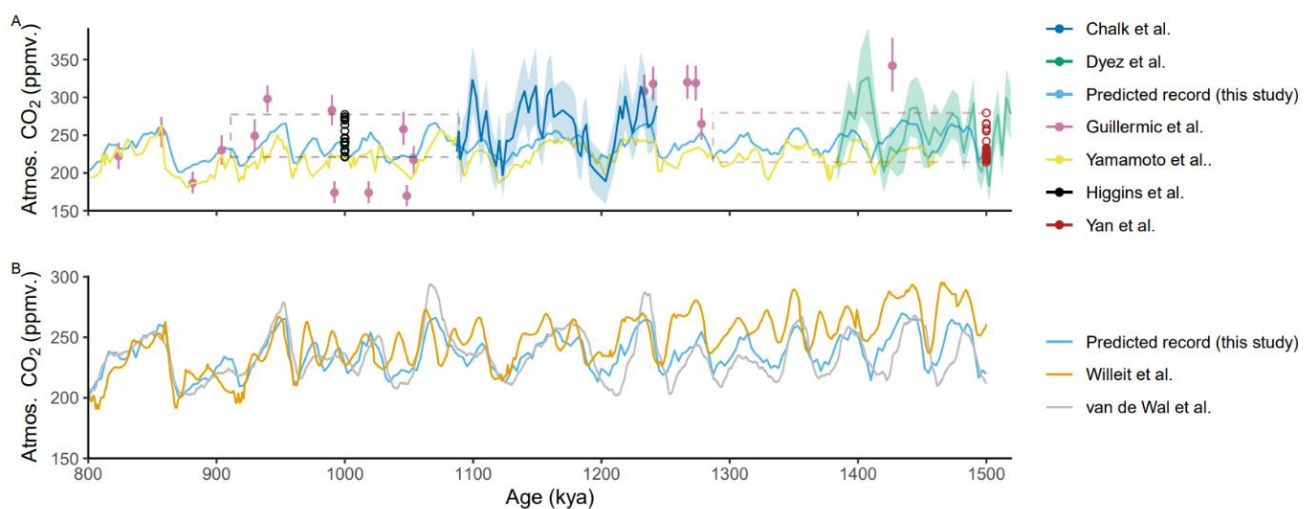
322 By comparison, the $\delta^{13}\text{C}$ of leaf wax data (Yamamoto *et al.*, 2022) has a similar glacial to interglacial range as
323 PRED-CO₂, but a ca. 20ppm lower mean concentration than our predictions (Fig 4A). Hence, our PRED-CO₂
324 data fall lower than interglacial $\delta^{11}\text{B}$ -based interglacial levels but are higher than the $\delta^{13}\text{C}$ of leaf-wax based
325 estimate. Given the evidence that $\delta^{11}\text{B}$ -based reconstructions are known to overestimate atmospheric CO₂

326 concentration in the continuous ice core record, we do not find cause from the existing CO₂ proxy data to reject
327 our predictions nor our associated null-hypothesis.

328

329 We also compare our predictions to existing more complex model simulations (Fig 4B.). First, against a
330 transient simulation using an intermediate-complexity earth system model (CLIMBER-2) by Willeit *et al.*
331 (2019). This study suggests a combination of gradual regolith removal and atmospheric CO₂ decline can explain
332 the long-term climate variability over the past 3Myr. Second, against a longer-term reconstruction by van de
333 Wal *et al.* (2011) that utilises deep-sea benthic isotope records to reconstruct a continuous CO₂ record over the
334 past 20 Myr. Our simple GLS model demonstrates a similar long-term trend and timing of glacial-interglacial
335 signals and an atmospheric CO₂ level that sits approximately mid-way between the two more complex models.

336



337

338 **Figure 4: A) Predicted CO₂ (this work) compared to observed, proxy CO₂ estimates from a range of other**
339 **sources: $\delta^{11}\text{B}$ -based pCO₂ reconstructions and measurements by Dyez *et al.* (2018), Guillermic *et al.***
340 **(2022); Chalk *et al.*, (2017); blue ice CO₂ measurements by Yan *et al.* (2019) and Higgins *et al.* (2015);**
341 **$\delta^{13}\text{C}$ leaf wax proxy reconstructions by Yamamoto *et al.* (2022). The dashed boxes indicate the dating**
342 **uncertainty and range of the respective BI-CO₂ records. B) Our predicted record compared to various**
343 **model simulations: a regolith removal hypothesis simulation by Willeit *et al.* (2019); and a high-resolution**
344 **CO₂ reconstruction by van de Wal *et al.* (2011)**

345

346 A complete and critical test of our and other CO₂ predictions awaits the upcoming analysis of the continuous
347 oldest ice core records. We now discuss some potential applications of the PRED-CO₂ record for hypothesis
348 testing on the cause of the MPT.

349

350 PRED-CO₂ shows a long-term decline in glacial CO₂ across the MPT, but no long-term decrease in interglacial
351 CO₂. This pattern is consistent with the boron-isotope-based CO₂ reconstructions shown earlier, where it is often
352 described as an increase in the interglacial to glacial CO₂ difference (e.g., Chalk *et al.*, 2017; Hönlisch *et al.*,
353 2009). Chalk *et al.* (2017) concludes that the MPT was initiated by a change in ice sheet dynamics and that
354 longer and higher-ice volume post-MPT ice ages are sustained by carbon cycle feedbacks, in particular dust
355 fertilization of the Southern Ocean. That fact that our LR04-based prediction of CO₂ captures this same trend, of

356 declining glacial CO₂, reflects that LR04 benthic stack also features an increase in the interglacial to glacial
357 benthic δ¹⁸O difference across the MPT, which is dominated by the glacial decline (Fig 3A.). Here, a
358 comparison of PRED-CO₂ to a realised continuous oldest ice core record will be of value. The agreement or
359 disagreement would inform on the proportionality of the CO₂ coupling with ice volume; if there were a major
360 new or non-linear process across the MPT that changed the nature of coupling between CO₂ and ice volume the
361 PRED-CO₂ and observed CO₂ records would be expected to diverge.

362

363 Another avenue to use the PRED-CO₂ record for hypothesis testing on the cause of the MPT concerns the phase
364 locking hypothesis. The phase locking hypothesis is proposed to explain the absence of precession-related (23
365 kyr) periods in the LR04 benthic stack prior to the MPT (Fig 1), despite the strong precession cycle in insolation
366 (Raymo *et al.*, 2006, Morée *et al.*, 2021). The key concept is that prior to the MPT the Northern Hemisphere and
367 Antarctic ice sheets were responsive (in ice volume) to insolation changes in the precession band, but because
368 precession forcing is out of phase between the hemispheres, the ice volume changes were opposing between the
369 hemispheres and therefore cancelled in the benthic stack. This cancellation of the precession signal left
370 insolation forcing in the 41 kyr obliquity band to dominate globally integrated ice volume changes expressed in
371 the benthic stack. A transition from a smaller and more dynamic terrestrial-terminating Antarctic ice sheet to a
372 larger and more stable marine-terminating ice sheet with cooling climate across the MPT (e.g. Elderfield *et al.*,
373 2012) is then proposed to remove sensitivity of Antarctic ice volume to precession forcing and to suppress ice
374 sheet sensitivity to the obliquity band in favour of quasi-100kyr ice volume changes that are in phase between
375 the hemispheres (Raymo *et al.*, 2006).

376

377 Recently presented data from Yan *et al.* (2022), lend some support to the phase locking hypothesis, specifically
378 with evidence that pre-MPT Antarctic temperature (and by extension ice volume) is positively correlated with a
379 local precession-band insolation proxy based on the oxygen to nitrogen ratio of trapped air (Yan *et al.*, 2022).
380 Whereas the correlation becomes negative in the blue ice and continuous ice core data in the post-MPT record.
381 If Yan *et al.*, (2022) is correct and the phase locking hypothesis holds, then an implication is that prior to the
382 MPT, Antarctic climate, Antarctic ice volume and by extension Southern Ocean climate conditions, would fall
383 out of phase with the LR04 benthic stack. To now extend the argument to potential impacts on CO₂ exchange, if
384 the phase locking hypothesis holds, then prior to the MPT the Antarctic and Southern Ocean climate conditions
385 and by extension the Southern Ocean mechanisms of CO₂ exchange described earlier, would also be expected to
386 fall out of phase with the benthic stack. Since our regression model assumes continuation of the in-phase
387 relationship between the benthic stack and Antarctic and Southern Ocean climate conditions (as inherited from
388 the post-MPT training data) we would expect to see major disagreement between our pre-MPT CO₂ predictions
389 and a realised oldest ice continuous ice core CO₂ record.

390

391 **5 Summary and Conclusions**

392 In this study we have used a simple generalised least squares (GLS) model to predict atmospheric CO₂ from the
393 LR04 benthic δ¹⁸O stack for the period spanning the mid-Pleistocene transition, 800–1500 kyr. Our CO₂
394 prediction is therefore based on the assumption that the physical processes linking CO₂, sea level, global ice
395 volume and ocean temperature over the past 800 kyr do not fundamentally change across the 800–1500 kya time

396 period. The null-hypothesis is deliberately simplistic on the basis that differences between our predictions and
397 observed or proxy CO₂ records may be revealing of the physical processes involved in the mid-Pleistocene
398 Transition.
399 We made initial tests of the null hypothesis by comparing our predicted CO₂ record to existing discrete blue ice
400 CO₂ records and other non-ice-core proxy-CO₂ records from the 800–1500 kyr interval. Our predicted CO₂
401 concentrations do not show any systematic departure from observed blue ice CO₂ concentrations. The
402 predictions are marginally lower (during glacial *and* interglacial stages) than those observed in blue ice from
403 1000 ± 89 kya and marginally higher than observed in blue ice data from 1.5 Mya ± 213 kyr. Our predictions
404 were generally lower than interglacial δ¹¹B-based-CO₂ reconstructions, but higher than recent δ¹³C of leaf-wax
405 based CO₂ reconstructions. Overall, we do not find clear evidence from the existing blue ice or proxy CO₂ data
406 to reject our predictions nor our associated null-hypothesis. The definitive test of our and other CO₂ predictions
407 therefore awaits the future analysis of the upcoming continuous oldest ice core records. The PRED-CO₂ record
408 presented here should provide a useful comparison to forthcoming oldest ice core records and opportunity to
409 provide further constraints on the processes involved in the MPT.

410

411 **Author contributions**

412 Project design by JRWM, JBP and TRV. Data analysis and writing led by JRWM with contributions from all
413 authors.

414

415 **Competing interests**

416 The authors declare that they have no competing interests.

417

418 **Disclaimer**

419 This study, to the best of the author(s) knowledge and belief, contains no material previously published or
420 written by another person, except where due reference is made in the text of the study.

421

422 **Acknowledgements**

423 We acknowledge assistance from Simon Wotherspoon (Institute for Marine and Antarctic Studies) in
424 appropriate model selection methods. This research was supported by the Australian Government through
425 Australian Antarctic Science projects 4632, the Million Year Ice Core (MYIC) Project and by the Australian
426 Government Department of Industry Science Energy and Resources, grant ASCI000002.

427

428 **Data availability**

429 PRED-CO₂ data will be publicly archived at the Australian Antarctic Data Centre (<https://data.aad.gov.au/>
430 >>full link provided upon publication<<).

431

432 **References**

- 433 Archer, D., Winguth, A., D. Lea, and Mahowald, N.: What caused the glacial/interglacial atmospheric
434 pCO₂ cycle?, *Rev. Geophys.*, 38, 159–189, 2000, <https://doi.org/10.1029/1999RG000066>, 2000.
435
436 Bazin, L., Landais, A., Lemieux-Dudon, B., Toye Mahamadou Kele, H., Veres, D., Parrenin, F., Martinerie, P.,
437 Ritz, C., Capron, E., Lipenkov, V., Loutre, M.-F., Raynaud, D., Vinther, B., Svensson, A., Rasmussen, S.,

438 Severi, M., Blunier, T., Leuenberger, M., Fischer, H., Masson-Delmotte, V., Chappellaz, J., and Wolff, E.: An
439 optimized multi-proxies, multi-site Antarctic ice and gas orbital chronology (AICC2012): 120-800 ka, *Clim.*
440 *Past*, 9, 1715-1731, <https://doi.org/10.5194/cp-9-1715-2013>, 2013.

441
442 Bereiter, B., Eggleston, S., Schmitt, J., Nehrbass-Ahles, C., Stocker, T. F., Fischer, H., Kipfstuhl, S., and
443 Chappellaz, J.: Revision of the EPICA Dome C CO₂ record from 800 to 600 ky before present, *Geophys. Res.*
444 *Let.*, 42, 542-549, <https://doi.org/10.1002/2014gl061957>, 2015.

445
446 Berends, C. J., de Boer, B., and van de Wal, R. S. W.: Reconstructing the evolution of ice sheets, sea level, and atmospheric
447 CO₂ during the past 3.6 million years. *Clim. Past*, 17, 361–377, <http://doi.org/10.5194/cp-17-361-2021>, 2021a.

448
449 Berends, C. J., Köhler, P., Lourens, L. J., and van de Wal, R. S. W.: On the cause of the mid-Pleistocene
450 transition., *Rev. Geophys.*, 59, e2020RG000727. <https://doi.org/10.1029/2020RG000727>, 2021b.

451
452 Berger, A., Li, X. S., and Loutre, M. F.: Modelling northern hemisphere ice volume over the last 3Ma,
453 *Quaternary. Sci. Rev.*, 18, 1-11, [https://doi.org/10.1016/S0277-3791\(98\)00033-X](https://doi.org/10.1016/S0277-3791(98)00033-X), 1999.

454
455 Broecker, W.S.: Glacial to interglacial changes in ocean chemistry, *Prog. Oceanogr.*, 11 (2), 151-197.
456 [https://doi.org/10.1016/0079-6611\(82\)90007-6](https://doi.org/10.1016/0079-6611(82)90007-6), 1982.

457
458 Chalk, T., Hain, M., Foster, G., Rohling, E., Sexton, P., Badger, M., Cherry, S., Hasenfratz, A., Haug, G.,
459 Jaccard, S., Martínez-García, A., Pälike, H., Pancost, R., and Wilson, P.: Causes of ice age intensification across
460 the Mid-Pleistocene Transition, *P. Natl. Acad. Sci. USA.*, 114, 13114-13119,
461 <https://doi.org/10.1073/pnas.1702143114>, 2017.

462
463 Clark, P. U., Archer, D., Pollard, D., Blum, J. D., Rial, J. A., Brovkin, V., Mix, A. C., Piasias, N. G., and Roy,
464 M.: The middle Pleistocene transition: characteristics, mechanisms, and implications for long-term changes in
465 atmospheric pCO₂, *Quat. Sci. Rev.*, 25, 3150-3184, <https://doi.org/10.1016/j.quascirev.2006.07.008>, 2006.

466
467 Clark, P. U. and Pollard, D.: Origin of the Middle Pleistocene Transition by ice sheet erosion of regolith,
468 *Paleoceanography*, 13, 1-9, <https://doi.org/10.1029/97pa02660>, 1998.

469
470 Dyez, K.A., Hönlisch, B., and Schmidt, G.A.: Early Pleistocene obliquity-scale pCO₂ variability at ~1.5 million
471 years ago. *Paleoceanogr. Paleoclimatol.*, 33, no. 11, 1270-1291, <https://doi.org/10.1029/2018PA003349>, 2018.

472
473 Elderfield, H., Ferretti, P., Greaves, S., Crowhurst, S., McCave, N., and Piotrowski, A.M.: Evolution of Ocean
474 Temperature and Ice Volume Through the Mid-Pleistocene Climate Transition, *Science*, 337,704-709,
475 <https://doi.org/10.1126/science.1221294>, 2012.

476
477 Gottschalk, J., Battaglia, G., Fischer, H., Frölicher, T.L., Jaccard, S.L., Jeltsch-Thömmes, A., Joos, F., Köhler,
478 P., Meissner, K.J., Menviel, L., Nehrbass-Ahles, C., Schmitt, J., Schmittner, A., Skinner, L.C., and Stocker,
479 T.G.: Mechanisms of millennial-scale atmospheric CO₂ change in numerical model simulations, *Quaternary.*
480 *Sci. Rev.*, 220, 30-74, <https://doi.org/10.1016/j.quascirev.2019.05.013>, 2019.

481
482 Guillermic, M., Misra, S., Eagle, R., and Tripathi, A.: Atmospheric CO₂ estimates for the Miocene to Pleistocene
483 based on foraminiferal $\delta^{11}\text{B}$ at Ocean Drilling Program Sites 806 and 807 in the Western Equatorial Pacific,
484 *Clim. Past*, 18(2), 183-207, <https://doi.org/10.5194/cp-18-183-2022>, 2022.

485
486 Hasenfratz, A. P., Jaccard, S. L., Martínez-García, A., Sigman, D. M., Hodell, D. A., Vance, D., Bernasconi, S.
487 M., Kleiven, H. F., Haumann, F. A., and Haug, G. H.: The residence time of Southern Ocean surface waters and
488 the 100,000-year ice age cycle, *Science*, 363, 1080, <https://doi.org/10.1126/science.aat7067>, 2019.

489
490 Higgins, J. A., Kurbatov, A. V., Spaulding, N. E., Brook, E., Introne, D. S., Chimiak, L. M., Yan, Y.,
491 Mayewski, P. A., and Bender, M. L.: Atmospheric composition 1 million years ago from blue ice in the Allan
492 Hills, Antarctica, *P. Natl. Acad. Sci. USA.*, 112, 6887, <https://doi.org/10.1073/pnas.1420232112>, 2015.

493
494 Hönlisch, B., Hemming, N. G., Archer, D., Siddall, M., and McManus, J. F.: Atmospheric Carbon Dioxide
495 Concentration Across the Mid-Pleistocene Transition, *Science*, 324, 1551,
496 <https://doi.org/10.1126/science.1171477>, 2009.

497

498 International Panel on Climate Change: Climate change 2001; IPCC third assessment report, IPCC, Geneva,
499 2001.
500

501 International Partnerships in Ice Core Sciences: The oldest ice core: A 1.5 million year record of climate and
502 greenhouse gases from Antarctica [White paper]. [https://igbp-](https://igbp-scor.pages.unibe.ch/sites/default/files/download/docs/working_groups/ipics/white-papers/ipics_oldaa_final.pdf)
503 [scor.pages.unibe.ch/sites/default/files/download/docs/working_groups/ipics/white-papers/ipics_oldaa_final.pdf](https://igbp-scor.pages.unibe.ch/sites/default/files/download/docs/working_groups/ipics/white-papers/ipics_oldaa_final.pdf),
504 accessed 06/12/2023, 2020.
505

506 Jouzel, J., Masson-Delmotte, V., Cattani, O., Dreyfus, G., Falourd, S., Hoffmann, G., Minster, B., Nouet, J.,
507 Barnola, J. M., Chappellaz, J., Fischer, H., Gallet, J. C., Johnsen, S., Leuenberger, M., Loulergue, L., Luethi, D.,
508 Oerter, H., Parrenin, F., Raisbeck, G., Raynaud, D., Schilt, A., Schwander, J., Selmo, E., Souchez, R., Spahni,
509 R., Stauffer, B., Steffensen, J. P., Stenni, B., Stocker, T. F., Tison, J. L., Werner, M., and Wolff, E. W.: Orbital
510 and Millennial Antarctic Climate Variability over the Past 800,000 Years, *Science*, 317, 793,
511 <https://doi.org/10.1126/science.1141038>, 2007.
512

513 Lisiecki, L. E. and Raymo, M. E.: A Pliocene-Pleistocene stack of 57 globally distributed benthic $\delta^{18}\text{O}$ records,
514 *Paleoceanography*, 20, PA1003, <https://doi.org/10.1029/2004pa001071>, 2005.
515

516 Martínez-García, A., Sigman, D.M., Ren, H., Anderson, R.F., Straub, M., Hodell, D.A., Jaccard, S.L., Eglinton,
517 T.I., and Haug, G.H.: Iron fertilization of the subantarctic ocean during the last ice age, *Science*, 343 (6177),
518 1347-1350, <https://doi.org/10.1126/science.1246848>, 2014.
519

520 McClymont, E.L., Sostdian, S.M., and Rosell-Melé, A.: Pleistocene sea-surface temperature evolution: Early
521 cooling, delayed glacial intensification, and implications for the mid-Pleistocene transition. *Earth. Sci. Rev.*,
522 123, 173-193, <https://doi.org/10.1016/j.earscirev.2013.04.006>, 2013.
523

524 Millero, F. J.: Thermodynamics of the carbon dioxide system in the oceans, *Geochim. Cosmochim. Acta.*, 59,
525 661-677, [https://doi.org/10.1016/0016-7037\(94\)00354-O](https://doi.org/10.1016/0016-7037(94)00354-O), 1995.
526

527 Morée, A. L., Sun, T., Bretones, A., Straume, E. O., Nisancioglu, K., and Gebbie, G.: Cancellation of the
528 precessional cycle in $\delta^{18}\text{O}$ records during the Early Pleistocene. *Geophys. Res. Lett.*, 48,
529 e2020GL090035. <https://doi.org/10.1029/2020GL090035>, 2021.
530

531 Petit, J. R., Jouzel, J., Raynaud, D., Barkov, N. I., Barnola, J. M., Basile, I., Bender, M., Chappellaz, J., Davis,
532 M., Delaygue, G., Delmotte, M., Kotlyakov, V. M., Legrand, M., Lipenkov, V. Y., Lorius, C., Pépin, L., Ritz,
533 C., Saltzman, E., and Stievenard, M.: Climate and atmospheric history of the past 420,000 years from the
534 Vostok ice core, Antarctica, *Nature*, 399, 429-436, <https://doi.org/10.1038/20859>, 1999.
535

536 Raymo, M., Lisiecki, L., and Nisancioglu, K.: Plio-Pleistocene Ice Volume, Antarctic Climate, and the Global
537 18O Record, *Science*, 313, 492-495, <https://doi.org/10.1126/science.1123296>, 2006.
538

539 Raymo, M., Ruddiman, W., and Froelich, P.: Influence of Late Cenozoic mountain building on ocean
540 geochemical cycles, *Geology*, 16, 649-653, [https://doi.org/10.1130/0091-](https://doi.org/10.1130/0091-7613(1988)016<0649:IOLCMB>2.3.CO;2)
541 [7613\(1988\)016<0649:IOLCMB>2.3.CO;2](https://doi.org/10.1130/0091-7613(1988)016<0649:IOLCMB>2.3.CO;2), 1988.
542

543 Raymo, M. E.: The timing of major climate terminations, *Paleoceanography*, 12, 577-585,
544 <https://doi.org/10.1029/97PA01169>, 1997.
545

546 Raymo, M. E. and Huybers, P.: Unlocking the mysteries of the ice ages, *Nature*, 451, 284-285,
547 <https://doi.org/10.1038/nature06589>, 2008.
548

549 Röthlisberger, R., Bigler, M., Wolff, E. W., Joos, F., Monnin, E., and Hutterli, M. A.: Ice core evidence for the
550 extent of past atmospheric CO_2 change due to iron fertilisation, *Geophys. Res. Lett.*, 31, L16207,
551 <https://doi.org/10.1029/12004GL020338>, 2004.
552

553 Ruddiman, W. F., Raymo, M. E., Martinson, D. G., Clement, B. M., and Backman, J.: Pleistocene evolution:
554 Northern hemisphere ice sheets and North Atlantic Ocean, *Paleoceanography*, 4, 353-412,
555 <https://doi.org/10.1029/PA004i004p00353>, 1989.
556

557 Shackleton, N. J. and Pisias, N. G.: Atmospheric Carbon Dioxide, Orbital Forcing, and Climate. In: The Carbon
558 Cycle and Atmospheric CO₂: Natural Variations Archean to Present, <https://doi.org/10.1029/GM032p0303>,
559 1985.

560

561 Shugi, H., The older the ice, the better the science. *Adv. Polar Sci.*, 23, 121-122,
562 <https://doi.org/10.13679/j.advps.2022.0004>, 2022.

563

564 Stephens, B.B., Keeling, R.F.: The influence of Antarctic sea ice on glacial–interglacial CO₂ variations. *Nature*,
565 404, 171–174, <https://doi.org/10.1038/35004556>, 2000.

566

567 Tzedakis, P. C., Crucifix, M., Mitsui, T., and Wolff, E. W.: A simple rule to determine which insolation cycles
568 lead to interglacials, *Nature*, 542, 427-432, <https://doi.org/10.1038/nature21364>, 2017.

569

570 Ushie, H., and Matsumoto, K.: The role of shelf nutrients on glacial-interglacial CO₂: A negative
571 feedback, *Global Biogeochem. Cy.*, 26, GB2039, <https://doi.org/10.1029/2011GB004147>., 2012.

572

573 van de Wal, R. S. W., de Boer, B., Lourens, L. J., Köhler, P., and Bintanja, R.: Reconstruction of a continuous
574 high-resolution CO₂ record over the past 20 million years. *Clim. Past*, 7, 1459–1469. [https://doi.org/10.5194/cp-](https://doi.org/10.5194/cp-7-1459-2011)
575 7-1459-2011, 2011.

576

577 Veres, D., Bazin, L., Landais, A., Toyé Mahamadou Kele, H., Lemieux-Dudon, B., Parrenin, F., Martinerie, P.,
578 Blayo, E., Blunier, T., Capron, E., Chappellaz, J., Rasmussen, S., Severi, M., Svensson, A., Vinther, B., and
579 Wolff, E.: The Antarctic ice core chronology (AICC2012): an optimized multi-parameter and multi-site dating
580 approach for the last 120 thousand years, *Clim. Past*, 9, 1733-1748, <https://doi.org/10.5194/cp-9-1733-2013>,
581 2013.

582

583 Willeit, M., Ganopolski, A., Calov, R., and Brovkin, V.: Mid-Pleistocene transition in glacial cycles explained by
584 declining CO₂ and regolith removal, *Sci. Adv.*, 5, eaav7337, doi: 10.1126/sciadv.aav7337, 2019.

585

586 Wolff, E. W., Chappella, J., Fischer, H., Kull, C., Miller, H., Stocker, T. F., and Watson, A. J.: The EPICA
587 challenge to the Earth system modeling community, *EOS*, 85, 363363, <https://doi.org/10.1029/2004EO380003>,
588 2004.

589

590 Wolff, E. W., Kull, C., Chappellaz, J., Fischer, H., Miller, H., Stocker, T. F., Watson, A. J., Flower, B., Joos, F.,
591 Köhler, P., Matsumoto, K., Monnin, E., Mudelsee, M., Paillard, D., and Shackleton, N.: Modeling past
592 atmospheric CO₂: results of a challenge, *EOS*, 86 (38), 341-345, <http://doi.org/10.1029/2005EO380003>, 2005.

593

594 Yamamoto, M., Clemens, S.C., Seki, O., Tsuchiya, Y., Huang, Y., O’ishi, R., and Abe-Ouchi, A.: Increased
595 interglacial atmospheric CO₂ levels followed the mid-Pleistocene Transition, *Nat. Geosci.*, 15(4), 307–313,
596 <https://doi.org/10.1038/s41561-022-00918-1>, 2022.

597

598 Yan, Y., Bender M.I., Brook, E.J., Clifford, H.M., Kemeny, P.C., Kurbatov, A.V., Mackay, S., Mayewski,
599 P.A., Ng, J., Severinghaus J.P., and Higgins, J.A.: Two-million-year-old snapshots of atmospheric gases from
600 Antarctic ice, *Nature*, 574(7780), 663–666, <https://doi.org/10.1038/s41586-019-1692-3>, 2019.

601

602 Yan, Y., Kurbatov, A.V., Mayewski, P.A., Shackleton, S., and Higgins, J.A.: Early Pleistocene East Antarctic
603 temperature in phase with local insolation. *Nat. Geosci.*, 16, 50-55, [https://doi.org/10.1038/s41561-022-01095-](https://doi.org/10.1038/s41561-022-01095-x)
604 x, 2022.